37th Cement and Concrete Science Conference
11-12 September 2017
University College London

Characterisation of Magnetite Formed during the Corrosion Process by Raman Spectroscopy – A Review

T.W. Mi and Y. Bai
Department of Civil, Environmental and Geomatic Engineering, University College London

J.J. Wang
Centre for Research on Adaptive Nanostructures and Nanodevices, Trinity College Dublin

ABSTRACT

Since the observation of Raman effect, Raman spectroscopy has been rapidly developed for a wide range of applications. Apart from the biomedical diagnosis, chemistry process monitoring and other biochemical applications, corrosion products identification has been another important application of Raman spectroscopy. The Raman effect of most corrosion products has been well understood over the last 70 years, but most experiments focused on pure composition. Since the 2000s, some research groups from European countries employed Raman spectroscopy as the major technique to investigate the corrosion mechanism of steel reinforcement. This paper presents a detailed review of the development made in the past on characterising magnetite using Raman spectroscopy. Issues and future research needs are also discussed and proposed.

1. INTRODUCTION

The employment of Raman spectroscopy to distinguish various corrosion products has been investigated intermittently over the last 40 years. The potential of Raman spectroscopy for characterisation of the corrosion products has been well established [1-3]. The development of Raman spectroscopy and associated analytical applications since the observation of Raman effect [4] has been impressive, resulting in less sample preparation and completing more complex measurement tasks.

By comparing with IR Spectroscopy, Raman demonstrates a simpler and more precise ability for characterising corrosion products. However, situation was inverse a quarter century ago when the IR was seen more versatile than Raman [5]. Thanks to the development of Raman associated technology, such as excitation laser, confocal microscopy and charge-coupled device (CCD), Raman has been a more applicable technique than IR spectroscopy in terms of corrosion related research now. Additionally, the Raman spectroscopy preforms a lager band spacing and sharper peaks in comparison with IR spectra, which avoids overlapping of characteristic peaks [1, 6] and achieves more precise identification.

The corrosion products of reinforcement embedded in concrete mainly consist of Iron II (FeO and $Fe(OH)_2$), Iron II, III (Fe_3O_4) and Iron III (α, β, γ, δ-FeOOH, and α, γ-Fe_2O_3). Figure 1 briefly presents several major events in the history of Raman study on corrosion products. The Raman effect of corundum was conducted by Porto and Krishnan [7], which was assigned to α-Fe_2O_3 by completing more experiments three years later by Beattie and Gilson [8]. In 1974, vibration modes of Fe_3O_4 was first predicted by Verble [9]. Four years later, Thibeau et al. [1] published the first systematic Raman study on corrosion product. However, this study produced mainly fundamental and primary results with limited practical information. In 1983, δ-FeOOH was first observed by Raman spectroscopy [10]. Two years later, the 2nd systematic research of the Raman study on corrosion products was conducted by Nauer et al. [2], however, in which Raman effect of iron oxides were not reported. Although the technique of Raman spectroscopy has been mentioned in earlier paper [11] by Japanese research group, they first reported the Raman spectra of two main corrosion products, α and γ-FeOOH [12] in 1994. At the end of the 1990s, De Faria et al. [13] completed the 3rd systematic study, pointing out the sensitivity of corrosion products to high power laser. Afterwards, Raman spectroscopy was widely used as an effective technique to investigate different kinds of corrosion associated researches.

Although almost all corrosion products of iron have ever been investigated by Raman spectroscopy, in terms of characteristic peaks and associated assignment, a really detailed and precise summary is still absent in the history. The feasibility and effectivity of Raman spectroscopy in distinguishing the corrosion product have been well demonstrated. This paper presents a systematic and comprehensive on characterising magnetite with Raman spectroscopy. The characterisation of other corrosion products will be reviewed elsewhere.

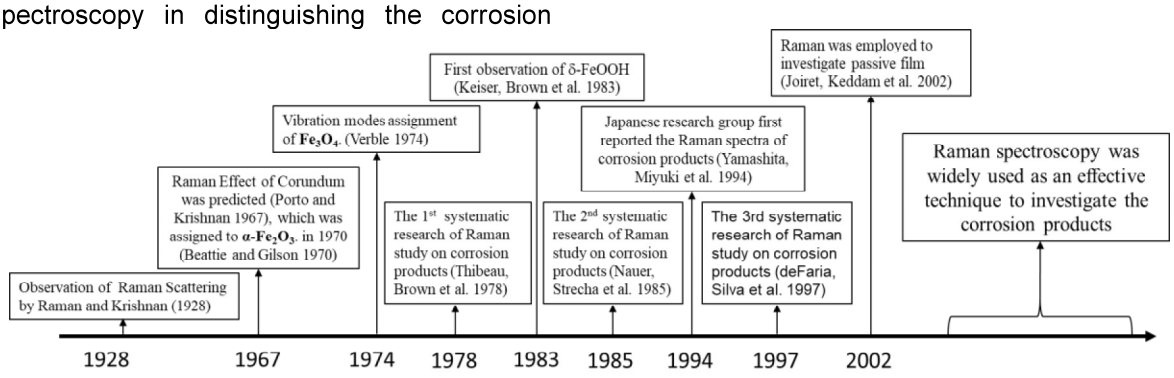

Figure 1 A summary of the development of Raman spectroscopy related to the corrosion products

2. MAGNETITE Fe_3O_4

Magnetite has been well understood over the last 100 years. It is in a typical structure of inverse spinel above the Verwey temperature (~120K), containing one divalent and two trivalent iron ions. As implied by the nature of inverse spinel structure (Figure 2), one iron(III) occupies the tetrahedral site (known as T sites) and the remaining Iron(III) and Iron(II) occupy the octahedral sites (known as M sites). The formula of magnetite, existing during the corrosion process, is thus $A^{3+}(B^{2+}A^{3+})\ O_4$, where A stands for trivalent ion and B for divalent ions. The exchange of electron in M sites results in a high conductivity property of magnetite.

Over half century's Raman study on magnetite, numerous experiments have confirmed the existence of five Raman-active modes, A_{1g}, E_g and three T_{2g} (Figure 3). The vibration modes were firstly predicted theoretically by White and DeAngelis [14] through a factor group analysis. Based on these results, Verble [9] studied the influence of temperature on the vibration modes of magnetite and then proposed an assignment for vibrational spectrum according to their experiment (Figure 3). But the transformation of magnetite was overlooked, where the peak at 420 cm^{-1} should be assigned to normal vibration mode E_g of hematite. Benefiting from the improvement of technology, many polarization studies on magnetite were conducted in these years and a more precise assignment was reported by Shebanova and Lazor [15] in 2003. By comparing different assignments, a strong agreement was made on the assignments of peaks at ~667 and ~536 cm^{-1}, which are related to vibrational mode A_{1g} and $T_{2g}(2)$ respectively (Table 1). According to depolarized Raman spectrum (Figure 4) from Shebanova and Lazor [15], E_g should be assigned to Raman peak at ~305 cm^{-1}. Consequently, three characteristic peaks at 667 cm^{-1} (A_{1g}), 536 cm^{-1} ($T_{2g}(2)$) and 305 cm^{-1} (E_g) are with the best agreement so far in literature.

An overview of the Raman frequencies in literature is presented in Table 2. Inspection of data indicates that Raman peaks at approximate 667cm^{-1}, 530cm^{-1} and 305cm^{-1} are most frequently observed. Especially for the Raman shift at ~667 cm^{-1}, it was reported by all authors mentioned in Table 2. The variations of Raman shifts for the same vibration modes are probably due to the differences in excitation laser used by different research groups. A higher shifts than 670 cm^{-1} is probably caused by the onset of a transformation from magnetite to hematite [15]. The characteristic peaks and relative assignment have been summarised in Table 1. A typical spectrum of magnetite is depicted in Figure 5, which also demonstrates that the Raman shift at ~667 cm^{-1} preforms the strongest intensity. In other words, the symmetric stretch of oxygen atoms along Fe-O bonds in T sites of magnetite occupy the majority of normal vibration modes.

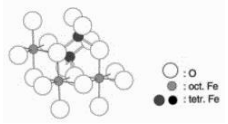

[16]

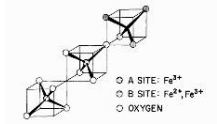

[9] A site =T site B site=M site

Figure 2. Cubic phase of magnetite

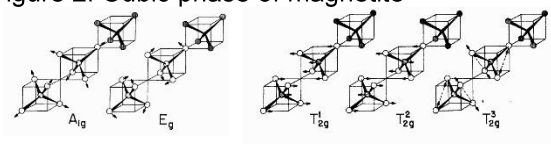

Figure 3. Diagrammatic representation of five normal vibration modes for magnetite (A_{1g} -

680cm^{-1},E_g - 420 cm^{-1}, T_{2g}(1) - 300 cm^{-1}, T_{2g}(2) - 560 cm^{-1}, T_{2g}(3) - 320 cm^{-1}) [9].

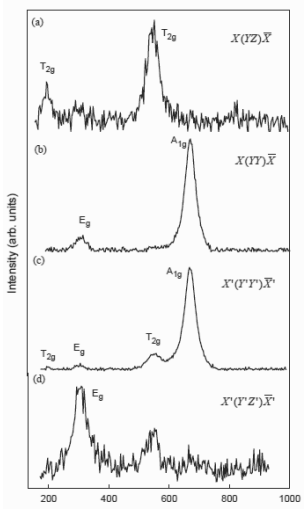

Figure 4. Depolarized study on magnetite

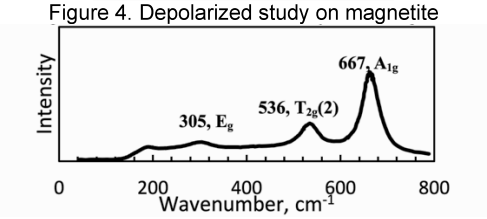

Figure 5. Representative Raman spectrum of magnetite based on Shebanova and Lazor [15]

Table 1. Raman vibrational modes for the characteristic peaks of magnetite

Compound	Raman shifts (cm^{-1})	Vibration Mode	Reference
Fe_3O_4	305	E_g - symmetric bends of Fe-O bonds	[15, 17]
	536	T_{2g}(2) - asymmetric stretch of Fe-O bonds	
	667	A_{1g} - symmetric stretch of oxygen atoms along Fe-O bonds in T sites	

Table 2. Raman frequencies reported in literature for magnetite

Reference	Raman shifts (cm-1)				
[1]*	663				
[3]	661	532		300	
[18]	667	532			
[19]	666	541		311	
[17]	670	540		308	193
[15]	668	538		306	193
[20]	670	540		310	
[21]	670	550		300	
[22]	670			306	
[6]	662	521		295	
[23]	680				
[24]	666				
[25]	660	530	382		
Average	667	536	-	305	-

*: Raman shift 616 cm^{-1} proposed by Thibeau et al. [1] is not listed because of the transformation of magnetite to hematite.

3. DISCUSSION AND CONCLUSION

Based on the information provided by this paper, identification of magnetite by Raman spectroscopy is feasible without any doubt. If the obtained spectrum demonstrates a strong peak at ~667 cm^{-1} and a second strongest peak at ~536 or 305 cm^{-1}, it obviously indicates the presence of magnetite. The remaining corrosion products can also be identified by Raman spectroscopy, indicating Raman spectroscopy is an effective technique to distinguish different corrosion products.

However, most of these works reported in the literature are based on the pure magnetite powder, which rarely happens in practice. The spectrum obtained from corrosion rust layer always represents a mixture of different corrosion products. Although there is no problem to characterise pure compounds according to the information presented in this paper, identifying a mixture is still a challenge in employing Raman spectroscopy for on-site work. Some research group from France have successfully employed Raman mapping to identify corrosion products [26-28], but there are still some issues need to be addressed, such as the accuracy of reference spectra and the scope of the application. Therefore, future studies are still needed to explore how to accurately identify the magnetite formed during the corrosion process of reinforcement in real world.

REFERENCES

[1]Thibeau, R.J., C.W. Brown, and R.H. Heidersbach, 1978, *Raman spectra of possible corrosion products of iron.* Applied Spectroscopy. **32**(6): p. 532-535.

[2]Nauer, G., et al., 1985, *Spectroscopic and thermoanalytical characterization of standard substances for the identification of reaction products on iron electrodes.* Journal of thermal analysis. **30**(4): p. 813-830.

[3]deFaria, D.L.A., S.V. Silva, and M.T. deOliveira, 1997, *Raman microspectroscopy of some iron oxides and oxyhydroxides.* Journal of Raman Spectroscopy. **28**(11): p. 873-878.

[4]Raman, C. and K. Krishnan, 1928, *A new type of secondary radiation (Reprinted from Nature, vol 121, pg 501-502, 1928).* Current Science. **74**(4): p. 381-381.

[5]Raman, A., B. Kuban, and A. Razvan, 1991, *The application of infrared spectroscopy to the study of atmospheric rust systems—I. Standard spectra and illustrative applications to identify rust phases in natural atmospheric corrosion products.* Corrosion Science. **32**(12): p. 1295-1306.

[6]Das, S. and M.J. Hendry, 2011, *Application of Raman spectroscopy to identify iron minerals commonly found in mine wastes.* Chemical Geology. **290**(3): p. 101-108.

[7]Porto, S. and R. Krishnan, 1967, *Raman effect of corundum.* The Journal of Chemical Physics. **47**(3): p. 1009-1012.

[8]Beattie, I. and T. Gilson, 1970, *The single-crystal Raman spectra of nearly opaque materials. Iron (III) oxide and chromium (III) oxide.* Journal of the Chemical Society A: Inorganic, Physical, Theoretical. p. 980-986.

[9]Verble, J.L., 1974, *Temperature-dependent light-scattering studies of the Verwey transition and electronic disorder in magnetite.* Physical Review B. **9**(12): p. 5236.

[10]Keiser, J.T., C.W. Brown, and R.H. Heidersbach, 1983, *Characterization of the passive film formed on weathering steels.* Corrosion Science. **23**(3): p. 251-259.

[11]Misawa, T., K. Hashimoto, and S. Shimodaira, 1974, *The mechanism of formation of iron oxide and oxyhydroxides in aqueous solutions at room temperature.* Corrosion Science. **14**(2): p. 131-149.

[12]Yamashita, M., et al., 1994, *The long term growth of the protective rust layer formed on weathering steel by atmospheric corrosion during a quarter of a century.* Corrosion Science. **36**(2): p. 283-299.

[13]De Faria, D., S. Venâncio Silva, and M. De Oliveira, 1997, *Raman microspectroscopy of some iron oxides and oxyhydroxides.* Journal of Raman spectroscopy. **28**(11): p. 873-878.

[14]White, W.B. and B.A. DeAngelis, 1967, *Interpretation of the vibrational spectra of spinels.* Spectrochimica Acta Part A: Molecular Spectroscopy. **23**(4): p. 985-995.

[15]Shebanova, O.N. and P. Lazor, 2003, *Raman spectroscopic study of magnetite (FeFe2O4): a new assignment for the vibrational spectrum.* Journal of Solid State Chemistry. **174**(2): p. 424-430.

[16]Cornell, R.M. and U. Schwertmann, 2003, *The iron oxides: structure, properties, reactions, occurrences and uses*. John Wiley & Sons.

[17]Gasparov, L.V., et al., 2000, *Infrared and Raman studies of the Verwey transition in magnetite.* Physical Review B. **62**(12): p. 7939-7944.

[18]Oh, S.J., D. Cook, and H. Townsend, 1998, *Characterization of iron oxides commonly formed as corrosion products on steel.* Hyperfine interactions. **112**(1-4): p. 59-66.

[19]Bersani, D., P.P. Lottici, and A. Montenero, 1999, *Micro-Raman investigation of iron oxide films and powders produced by sol-gel syntheses.* Journal of Raman Spectroscopy. **30**(5): p. 355-360.

[20]Hanesch, M., 2009, *Raman spectroscopy of iron oxides and (oxy)hydroxides at low laser power and possible applications in environmental magnetic studies.* Geophysical Journal International. **177**(3): p. 941-948.

[21]Jubb, A.M. and H.C. Allen, 2010, *Vibrational spectroscopic characterization of hematite, maghemite, and magnetite thin films produced by vapor deposition.* ACS Applied Materials & Interfaces. **2**(10): p. 2804-2812.

[22]Li, Y.-S., J.S. Church, and A.L. Woodhead, 2012, *Infrared and Raman spectroscopic studies on iron oxide magnetic nano-particles and their surface modifications.* Journal of Magnetism and Magnetic Materials. **324**(8): p. 1543-1550.

[23]Yohai, L., et al., 2016, *Phosphate ions as effective inhibitors for carbon steel in carbonated solutions contaminated with chloride ions.* Electrochimica Acta. **202**: p. 231-242.

[24]de la Fuente, D., et al., 2016, *Corrosion mechanisms of mild steel in chloride-rich atmospheres.* Materials and Corrosion-Werkstoffe Und Korrosion. **67**(3): p. 227-238.

[25]Morcillo, M., et al., 2016, *SEM/Micro-Raman Characterization of the Morphologies of Marine Atmospheric Corrosion Products Formed on Mild Steel.* Journal of the Electrochemical Society. **163**(8): p. C426-C439.

[26]Monnier, J., et al., 2011, *A methodology for Raman structural quantification imaging and its application to iron indoor atmospheric corrosion products.* Journal of Raman Spectroscopy. **42**(4): p. 773-781.

[27]Neff, D., et al., 2006, *Raman imaging of ancient rust scales on archaeological iron artefacts for long-term atmospheric corrosion mechanisms study.* Journal of Raman Spectroscopy. **37**(10): p. 1228-1237.

[28]Bouchar, M., et al., 2013, *The complex corrosion system of a medieval iron rebar from the Bourges' Cathedral. Characterization and reactivity studies.* Corrosion Science. **76**: p. 361-372.